Published in final edited form as:
J Neurochem. 2010 January 1; 112(1): 24–33. doi:10.1111/j.1471-4159.2009.06428.x.

In Vivo Neurochemical Profiling of Rat Brain by ^{1}H-[^{13}C] NMR Spectroscopy. Cerebral Energetics and Glutamatergic/GABAergic Neurotransmission

Pieter van Eijsden[1], **Kevin L. Behar**[4], **Graeme F. Mason**[4], **Kees P.J. Braun**[2], and **Robin A. de Graaf**[3]

[1]Department of Neurosurgery, Rudolf Magnus Institute of Neuroscience, University Medical Center Utrecht, The Netherlands [2]Department of Child Neurology, Rudolf Magnus Institute of Neuroscience, University Medical Center Utrecht, The Netherlands [3]Department of Radiology, Magnetic Resonance Research Center, Yale University School of Medicine, New Haven, Connecticut, USA [4]Department of Psychiatry, Magnetic Resonance Research Center, Yale University School of Medicine, New Haven, Connecticut, USA

Abstract

The simultaneous quantification of excitatory and inhibitory neurotransmission and the associated energy metabolism is crucial for a proper understanding of brain function. While the detection of glutamatergic neurotransmission *in vivo* by ^{13}C NMR spectroscopy is now relatively routine, the detection of GABAergic neurotransmission *in vivo* has remained elusive due to the low GABA concentration and spectral overlap. Using ^{1}H-[^{13}C] NMR spectroscopy at high magnetic field in combination with robust spectral modeling and the use of different substrates, [U-$^{13}C_6$]-glucose and [2-^{13}C]-acetate, it is shown that GABAergic, as well as glutamatergic neurotransmitter fluxes can be detected non-invasively in rat brain *in vivo*.

Keywords

GABA; ^{1}H-[^{13}C] NMR; glutamate; cerebral metabolism; rat

INTRODUCTION

Neurochemistry is concerned with the study of molecular and cellular processes of the nervous system and their relationship to function. Energy metabolism and neurotransmission are two crucial processes affecting almost all aspects of cerebral function. Proper characterization not only involves determination of absolute metabolite concentrations, but also requires knowledge of the dynamic metabolic turnover of the metabolites involved. ^{1}H NMR spectroscopy is currently the only technique that allows the non-invasive detection and quantification of a wide range of neurochemicals (Pfeuffer et al. 1999a). Direct ^{13}C (Behar et al. 1986; Beckmann et al. 1991; Gruetter et al. 1994) or indirect ^{1}H-observed, ^{13}C-edited (^{1}H-[^{13}C]) NMR spectroscopy (Rothman et al. 1985; Rothman et al. 1992) enables the dynamic detection of ^{13}C labeled product formation, like [4-^{13}C]-glutamate, [4-^{13}C]-glutamine and [2-^{13}C]-GABA, which are derived from intravenously infused, ^{13}C enriched substrates, such as

Corresponding Author: Robin A de Graaf, MRRC, Yale University, TAC, N145, 300 Cedar Street, New Haven, CT 06520-8043, USA, Tel: 203-785-6203, Fax: 203-785-6643, robin.degraaf@yale.edu.

[1-^{13}C]-glucose. ^{1}H-[^{13}C] NMR spectroscopy provides spectral information similar to the more traditional direct ^{13}C NMR spectroscopy approach, but with the higher sensitivity of proton detection.

Previously, ^{13}C and ^{1}H-[^{13}C] NMR spectroscopy have been used to study energy metabolism in the human (Rothman et al. 1992; Gruetter et al. 1994; Mason et al. 1995; Shen et al. 1999; Gruetter et al. 2001) and animal (Rothman et al. 1985; Fitzpatrick et al. 1990; Mason et al. 1992; Sibson et al. 1998; Sibson et al. 2001; de Graaf et al. 2003) brain during hibernating (Henry et al. 2007), resting (Rothman et al. 1985; Fitzpatrick et al. 1990; Mason et al. 1992; Rothman et al. 1992; Gruetter et al. 1994; Mason et al. 1995; Sibson et al. 1998; Shen et al. 1999; Gruetter et al. 2001; Sibson et al. 2001; de Graaf et al. 2003; Deelchand et al. 2009b; Deelchand et al. 2009a) and stimulated (Chen et al. 2001; Chhina et al. 2001; Patel et al. 2004) conditions. Glutamatergic neurotransmission has been assessed as a glutamate-glutamine neurotransmitter cycle between neurons and astroglia (Sibson et al. 1997). In addition, some of the smaller metabolic pathways like anaplerosis (Sibson et al. 2001; Mason et al. 2007) and astroglial energy metabolism (Bluml et al. 2002; Lebon et al. 2002) have been studied with alternate substrates, such as [2-^{13}C]-acetate and [2-^{13}C]-glucose. The results of ^{13}C MRS have been validated through the use of ^{18}F-FDG PET in the monkey brain (Boumezbeur et al. 2005). One of the most important findings from these studies was the linear correlation between increments of cerebral energy metabolism and total neurotransmitter cycling (Sibson et al. 1998). This relation was subsequently refined by separating the contributions of excitatory glutamatergic and inhibitory GABAergic neurotransmission. However, due to the low concentration of GABA and the strong spectral overlap with other metabolites and macromolecules, studies were necessarily performed *ex vivo* (Patel et al. 2005). Fortunately, with the availability of higher magnetic fields and the subsequent increase in spectral resolution and signal-to-noise ratio (SNR), the detection of lower-concentration metabolites, like GABA, became feasible. Several studies have qualitatively observed the formation of [3-^{13}C]-GABA following [1-^{13}C]-glucose or [1,6-$^{13}C_2$]-glucose infusion (Pfeuffer et al. 1999b; de Graaf et al. 2003; Deelchand et al. 2009b). However, due to limited SNR and/or spectral resolution, to date no studies have appeared that *quantitatively* assess the metabolic fluxes associated with GABA turnover in the normal rat brain *in vivo*. Yang et al. (Yang et al. 2007) were able to measure cerebral GABA turnover *in vivo*, but only after administration of a GABA-transaminase inhibitor to elevate GABA levels (Manor et al. 1996; de Graaf et al. 2006a).

The aim of the current study is to assess the extent to which ^{1}H-[^{13}C] NMR spectroscopy can provide reliable and quantifiable neurochemical information about brain metabolite concentrations and turnover under physiological conditions in rat brain *in vivo* at 9.4 T. In particular, the ability to *quantitatively* determine metabolic fluxes of GABA, as well as glutamate, *in vivo* will be established. The simultaneous detection of excitatory and inhibitory neurotransmission and cerebral energetics should provide a valuable, non-invasive tool in the understanding of brain function.

METHODS

Animal preparation

Animal experiments were conducted in accordance with federal guidelines on the care and use of laboratory animals under approved protocols by the Yale Animal Care and Use Committee.

Following an overnight fast (12-16 hours) ten Wistar rats (165.6 ± 12.0 g, mean ± SD) were anaesthetized with 2-3% halothane in a mixture of N_2O and O_2 (70/27-28%), tracheotomized and ventilated. A femoral artery was cannulated for monitoring of mean arterial blood pressure (MAP) and blood sampling to determine arterial blood gasses (pCO_2 and pO_2) and pH. Small

adjustments in tidal volume and ventilation frequency kept these physiological variables within normal limits (pCO_2 = 33–45 mm Hg; $pO_2 \geq 120$ mm Hg; pH = 7.30–7.58; MAP = 90–110 mm Hg). Body core temperature was measured with a rectal thermometer and maintained at 37 ± 1°C by means of a heated water pad. A femoral vein was cannulated for infusion of [U-$^{13}C_6$]-glucose (Glc, n = 5) or [2-^{13}C]-acetate (Ace, n = 5; Cambridge Isotope Laboratories Inc, Andover, MA). Briefly, animals received an initial 250 μL intravenous bolus of 0.75 M [U-$^{13}C_6$]-glucose (per 200 gram body weight) followed by an intravenous infusion of 0.75 M [U-$^{13}C_6$]-glucose. The infusion rate was decreased manually every 30 s according to a decreasing exponential function during the first 8 min and was constant at 13.7 μL/min for the remainder of the experiment. For acetate, animals received an initial 200 μL intravenous bolus of 2.0 M [2-^{13}C]-acetate over 15 s. The infusion rate was decreased to 50 and 25 μL/min at 15 s and 240 s, respectively, and remained constant at 12.5 μL/min for the remainder of the experiment (t > 480 s). Following surgery, halothane was reduced to 0.5 – 1% to maintain a stable blood pressure. Animal heads were shaven to allow for better coil positioning and animals were placed in the probe, restrained in a head holder and were further immobilized with d-tubocurarine (0.5 mg/kg/40 min, i.p.). After the magnetic resonance experiments, the rats were euthanized while still anaesthetized.

Magnetic resonance spectroscopy

Experiments were performed on a 9.4 T Magnex magnet and Bruker console (Bruker, Billerica, MA) equipped with a 9 cm diameter gradient coil insert (Resonance Research Inc, Billerica, MA, 490 mT/m in 175 μs). A 14 mm diameter surface coil was used for ^{1}H radio frequency (RF) pulse excitation and signal reception (400.5 MHz). RF pulse transmission on ^{13}C (100.2 MHz) was achieved with two orthogonal 21 mm diameter surface coils driven in quadrature (Adriany and Gruetter 1997). Multi-slice echo planar images (Field of view 2.56 × 2.56 cm, matrix 128 × 128, 10 slices of 1 mm thickness, repetition time (TR)/echo time (TE) = 2500/10 ms) were acquired and used to position the spectroscopic volume of interest (VOI) (6 × 5 × 6 mm) over the hippocampal area as close to the surface coil as possible, but remaining at least 0.5 mm away from the edges of the brain to improve magnetic field homogeneity. The rostralcaudal center of the voxel was positioned in the slice that showed the most dorsal portion of the medial hippocampus.

The magnetic field homogeneity over the VOI was optimized with the non-iterative, *F*ast *A*utomatic *S*himming *T*echnique by *M*apping *A*long *P*rojections (FASTMAP) for all first- and second-order shim coils (Gruetter 1993). This resulted in signal line widths of 14–16 Hz for water and 9–11 Hz for metabolites in the localized volume of 180 μL. Localized ^{1}H NMR spectra were obtained with the NMR pulse sequence described previously (de Graaf et al. 2003). In short, 3D localization was achieved by a combination of outer volume suppression, image-selected *in vivo* spectroscopy (ISIS), and slice-selective excitation. Water suppression was performed with *S*elective *W*ater suppression with *A*diabatic *M*odulated *P*ulses, SWAMP (de Graaf and Nicolay 1998), an adiabatic analog of the *CHE*mical *S*hift *S*elective, CHESS (Haase et al. 1985), technique. Discrimination between ^{1}H-[^{13}C] and ^{1}H-[^{12}C] NMR signals was achieved by executing a 4.0 ms adiabatic full passage (AFP) pulse (sin40 modulation, 10 kHz bandwidth, (Tannus and Garwood 1996)) on the ^{13}C channel on alternating acquisitions, after which the free induction decays (FIDs) obtained with and without the ^{13}C inversion were stored in separate memory blocks. ^{1}H-[^{13}C] NMR signals were obtained by subtraction of the ^{13}C-inverted FIDs from the non-inverted FIDs. Broadband adiabatic ^{13}C decoupling was applied during the total acquisition time of 204.8 ms. The decoupling sequence was executed with a 1.6 ms AFP pulse (HS4 modulation, 6.25 kHz bandwidth, (Tannus and Garwood 1996)) incorporated in a 20-step supercycle (Fujiwara and Nagayama 1988) to provide adiabatic, frequency-selective decoupling (de Graaf 2005). With the decoupling frequency centered on the [4-^{13}C]-glutamate resonance at 34.2 ppm, the decoupling sequence provides

frequency-selective decoupling between circa 3 and 65 ppm, while leaving the [1-^{13}C]-glucose resonances at 92.7 and 96.6 ppm unperturbed. Since the αH1-glucose resonance is resolved in ^{1}H NMR spectra at 9.4 T, frequency-selective decoupling allows for direct quantification of the ^{13}C fractional enrichment of cerebral glucose from total, unedited ^{1}H NMR spectra (de Graaf 2005).

The total GABA concentration was obtained through homonuclear spectral editing with a double spin-echo sequence using 20 ms Gaussian refocusing pulses selective for the GABA-H3 protons at 1.89 ppm (Mescher et al. 1998). An echo time of 68 ms (= 1/2*J*) was chosen to optimize the detection efficiency of the GABA-H4 protons at 3.01 ppm. RF pulse calibration was performed on the water resonance. Editing efficiency on individual animals was calculated from the residual water signal in the presence of spectral editing pulses. The experiments were performed with a repetition time TR of 4.0 s and 64 repetitions with interleaved editing. The GABA-edited spectrum was obtained by subtracting the non-edited from the edited spectra.

Data Acquisition and Processing

All FIDs were acquired with a 32 s time resolution (eight ISIS increments with TR = 4.0 s) to minimize the effects of small frequency shifts between acquisitions and to evaluate motion artifacts. Following a complete experiment of approximately 32 min of continuous signal acquisition, FIDs were zero-filled to 8 K data points, apodized (1.0 Hz Gaussian line broadening), Fourier transformed, and phase corrected (only zero-order phase). The spectra were frequency corrected to account for drift in the main magnetic field, but no amplitude or phase corrections were performed on individual spectra. Next, spectra acquired over 16 min were added to increase the SNR and used for subsequent quantification of metabolite concentrations and fractional enrichments by an in-house frequency-domain fitting program written in Matlab 7.0.4 (The Mathworks, Natick, MA). Similar to LCmodel (Provencher 1993), the algorithm models the *in vivo* NMR spectrum as a superposition of a basis set of *in vitro* NMR spectra of pure metabolite solutions. ^{1}H NMR spectra were collected *in vitro* under controlled pH and temperature conditions from acetate (Ace), alanine (Ala), aspartate (Asp), creatine (Cr), γ-aminobutyric acid (GABA), glucose (Glc), [U-$^{13}C_6$]-Glc, glutamate (Glu), glutamine (Gln), glutathione (GSH), glycerophosphorylcholine (GPC), lactate (Lac), *myo*-inositol (mI), *N*-acetyl aspartate (NAA), NAA-glutamate, phosphocreatine (PCr), phosphocholine (PC), phosphoethanolamine (PE), taurine (Tau) and valine (Val). A macromolecular baseline was measured separately on a number of animals by ‘nulling’ the metabolite resonances with a double inversion recovery element preceding the ^{1}H-[^{13}C] NMR sequence with 1.0 ms hyperbolic secant modulated AFP pulses (bandwidth 10 kHz), inversion recovery time TI = 1950 and 550 ms and TR = 6000 ms (de Graaf et al. 2006b). Following spectral fitting the absolute metabolite concentrations were calculated with respect to total creatine (tCr = PCr + Cr) under the assumption of a 10 mM tCr concentration. No correction for differential T_2 relaxation was performed. A separate version of the fitting program with additional constraints and a reduced basis set (Ace, Ala, Asp, GABA, Glc, Gln, Glu, Lac, NAA) was used for quantification of the edited ^{1}H-[^{13}C] NMR spectra. Specifically, while the resonance amplitudes of the different isotopically-labeled peaks within one molecule (e.g. [2-^{13}C], [3-^{13}C] and [4-^{13}C]-glutamate) were unconstrained, the line width, phase and frequency were forced to be identical. The reliability of the spectral fit was evaluated by Monte Carlo simulations (MCS) using 50 iterations. The traditional Cramer-Rao lower bounds (CRLBs) were not used, as they are not valid in the presence of an unknown macromolecular baseline. While the CRLBs can be modified to include so-called ‘nuisance’ parameters related to the baseline (Ratiney et al. 2005), we found the use of MCS a more straightforward alternative. The MCS results are expressed as the % (SD MCS/mean MCS), to indicate the percentage of uncertainty in the concentration that is determined from the spectral fitting.

Metabolic Modeling

To obtain the rates of the glutamatergic and GABAergic TCA cycles ($V_{TCA,Glu}$ and $V_{TCA,GABA}$) and the rates of glutamatergic and GABAergic neurotransmission ($V_{cycle,GluGln}$ and $V_{cycle,GABAGln}$), the study was designed with two different substrates, [U-$^{13}C_6$]-Glc and [2-^{13}C]-Ace. The dynamic [U-$^{13}C_6$]-Glc study provides information on $V_{TCA,Glu}$, $V_{TCA,GABA}$ and $V_{cycle,total} = V_{cycle,GluGln} + V_{cycle,GABAGln}$. The individual glutamatergic and GABAergic neurotransmitter cycling rates cannot be separated during a [U-$^{13}C_6$]-Glc study since both neurotransmission cycles label the same [4-^{13}C]-Gln position in the astroglial compartment (Patel et al. 2005). As detailed below, the steady-state [2-^{13}C]-Ace study is used to obtain the ratio between the neurotransmitter cycle rate and the TCA cycle rate for each neuronal compartment. This ratio is used as a constraint during the metabolic modeling of the dynamic [U-$^{13}C_6$]-Glc study in order to obtain all four independent rates, $V_{TCA,Glu}$, $V_{TCA,GABA}$, $V_{cycle,GluGln}$ and $V_{cycle,GABAGln}$.

Time courses for [3-^{13}C]-Glu, [4-^{13}C]-Glu, [3-^{13}C]-Gln, [4-^{13}C]-Gln, [2-^{13}C]-GABA and [4-^{13}C]-GABA were reconstructed over 16 min intervals during infusion of [U-$^{13}C_6$]-Glc. During the [2-^{13}C]-acetate infusion only the endpoint fractional enrichments were calculated. The glucose time courses were analyzed using a three-compartment metabolic model, comprising glutamatergic neuronal, GABAergic neuronal and astroglial compartments, similar to the model described by Patel et al (Patel et al. 2005). Briefly, blood glucose enters the brain via Michaelis-Menten-based transport across the blood-brain-barrier. However, since [1-^{12}C]-αH1-glucose and [1-^{13}C]-αH1-glucose levels could be detected and quantified directly in the brain compartment, no assumptions were required regarding glucose transport across the blood-brain barrier. Brain glucose is converted to pyruvate, which enters either the neuronal or astroglial tricarboxylic acid (TCA) cycles. The ^{13}C label of [U-$^{13}C_6$]-glucose will arrive at the TCA cycle intermediate [4-^{13}C]-ketoglutarate (KG), which is in rapid exchange with [4-^{13}C]-Glu at a rate V_x. Since [3-^{13}C]-Glu and [3-^{13}C]-Gln were both measured and included in the model, no assumptions about V_x were required. After labeling of [4-^{13}C]-Glu, the [4-^{13}C]-Gln position is ultimately labeled by the action of a glutamatergic neurotransmitter cycle between the glutamatergic neuronal and astroglial compartments. After one additional turn of the TCA cycle also [3-^{13}C]-Glu and [3-^{13}C]-Gln will label. In the GABAergic neuronal compartment, [4-^{13}C]-Glu is quickly converted to [2-^{13}C]-GABA, which ultimately labels [4-^{13}C]-Gln through a neurotransmitter cycle between the GABAergic neuron and the astroglial compartment. In a subsequent turn of the TCA cycle both [3-^{13}C]-GABA and [4-^{13}C]-GABA are labeled. Infusion of [2-^{13}C]-Ace will first label the small astroglial [4-^{13}C]-Glu pool, after which the label will appear in the larger astroglial [4-^{13}C]-Gln pool. Gln is subsequently shuttled from the astroglia to the neurons where it will label the [4-^{13}C]-Glu pools of both the GABAergic and glutamatergic compartments. Further details on the metabolic model can be found in (Patel et al. 2005).

In this metabolic model, a large set of coupled differential equations (using mass and isotope balance) was used within the CWave software package (Cwave 3.0, (Mason et al. 2003)) to describe the behavior of above mentioned labeled substrates in response to the infusion of [U-$^{13}C_6$]-glucose. This model was restricted by prior knowledge from the steady state [2-^{13}C] acetate experiment, from which the ratio between V_{cycle} and V_{TCA} can be determined for the glutamatergic and GABAergic compartment. For this, the differential equations that describe the flow of ^{13}C through the Glu/Gln and GABA/Gln cycles were solved analytically for the steady-state condition (Patel et al. 2005), which yielded the following relationships between V_{cycle} and V_{TCA} for glutamatergic and GABAergic neurons

$$V_{cycle,GluGln}/V_{TCA,Glu} = FE_{Glu4}/(FE_{Gln4} - FE_{Glu4}) \quad [1]$$

$$V_{cycle,GABAGln}/V_{TCA,GABA} = FE_{GABA2}/(FE_{Gln4} - FE_{GABA2}) \quad [2]$$

where FE_{Glu4}, FE_{Gln4} and FE_{GABA2} represent the steady state ^{13}C enrichments of these amino acids during the infusion of [2-^{13}C]-Ace.

The model was further constrained by assuming the pyruvate carboxylase flow (V_{pc}) to be 20% of the rate of total glutamine synthesis (Sibson et al. 2001). Dilutional fluxes were iterated for the three separate compartments. The cerebral metabolic rates were determined from the best fits of the model to the time-courses of ^{13}C labeling with a Levenberg-Marquardt algorithm hybridized with simulated annealing (Alcolea et al. 1999). Cerebral metabolic rates of glucose oxidation [$CMR_{Glc(ox)}$] were calculated as $½V_{TCA}$. The GABA pool was assigned to the GABAergic neuronal compartment, whereas Glu was divided between glutamatergic neurons (88%), astroglia (10%), and GABAergic neurons (2%) (Storm-Mathisen et al. 1983; Chaudhry et al. 1995). Gln was assumed to be synthesized in the astroglial compartment and degraded in the neuronal compartment.

With the described prior knowledge and restrictions, the metabolic model was used to determine the glutamatergic neuronal TCA cycle rate ($V_{TCA,Glu}$), the GABAergic TCA cycle rate ($V_{TCA,GABA}$) and astroglial TCA cycle rate ($V_{TCA,A}$), the rate between α-KG and Glu (V_x), the glutamatergic neurotransmitter cycle rate ($V_{cycle,GluGln}$), the GABA shunt (V_{GABA}), the GABAergic neurotransmitter cycle rate ($V_{cycle,GABAGln}$) and the dilutional rates ($V_{dil,Glu}$, $V_{dil,Gln}$ and $V_{dil,GABA}$).

RESULTS

Fig. 1 shows a typical ^1H NMR spectrum from rat brain *in vivo* at 9.4 T acquired between 120 and 150 min following the start of intravenous [U-$^{13}C_6$]-glucose infusion. Fig 1C shows, besides the experimentally measured spectrum (top trace), the total spectral fit, the spectral contributions of glutamate, glutamine, GABA and lactate to the total fit, the macromolecular baseline and the difference between the measured and fitted spectra (bottom trace). The absolute metabolite concentrations are listed in Table 1. Since the adiabatic decoupling sequence provides frequency-selective decoupling (from circa 3 ppm to 65 ppm on the ^{13}C channel) all ^1H-[^{13}C] NMR resonances upfield from water are perfectly decoupled. Since the ^{13}C resonances from [1-^{13}C]-glucose fall outside the decoupling range, the ^1H resonances of [1-^{13}C]-αH1-glucose are not decoupled (Fig. 1A). The ^{13}C inversion pulse inverts the ^1H-[^{13}C] resonances relative to the ^1H-[^{12}C] resonances on subsequent scans. However, since the ^{13}C inversion pulse is also frequency-selective, the [1-^{13}C]-αH1-glucose resonances do not invert and are thus identical in the absence (upper trace) or presence (lower trace) of the ^{13}C editing pulse. Besides the excellent spectral fit, the most noticeable feature of Fig. 1C is the origin of the signal at 2.2 – 2.3 ppm as indicated by the dotted line. Even though this signal is commonly referred to as GABA-H2, it is clear from Fig. 1C that the majority of this signal must be assigned to macromolecules with only a minor, shifted contribution from GABA-H2. When the macromolecular baseline is properly accounted for, it has been shown that GABA can be accurately quantified from short-TE ^1H NMR spectra (Pfeuffer et al. 1999a). However, in the current study the obtained GABA concentration showed a clear deviation (0.50 ± 0.07 mM) from known GABA levels when calculated directly from the short TE ^1H NMR spectrum. As a result GABA detection was achieved with more conventional homonuclear spectral editing. Fig. 2 shows two ^1H NMR spectra with and without selective refocusing of GABA-H3. The difference between the two NMR spectra reveals the outer two resonances of the GABA-H4 triplet at 3.01 ppm. The finite bandwidth of the selective refocusing pulses leads

to partial co-editing of *N*-acetyl aspartate (NAA) at 2.01 ppm and glutamate/glutamine at 3.75 ppm. However, these resonance are well-separated from GABA-H4 and do not affect the GABA quantification. Due to the increased chemical shift dispersion at 9.4 T co-editing of macromolecules was minimal. The GABA concentration obtained through homonuclear spectral editing was 1.17 ± 0.31 mM.

Fig. 3 shows the edited ^{1}H-[^{13}C] NMR spectrum obtained from rat brain 120 min following the onset of the [U-$^{13}C_6$]-glucose infusion. The most prominent resonances originated from glutamate, glutamine and GABA. Note that all spectra were acquired in the presence of selective ^{13}C decoupling, thus eliminating splitting due to heteronuclear scalar coupling. The decoupling and editing pulses did not affect the [1-^{13}C]-α-glucose resonances at 92.7 ppm, such that (1) heteronuclear scalar coupling is still visible on the αH1-glucose resonance at 5.23 ppm and (2) [1-^{13}C]-αH1-glucose does not appear in the ^{1}H-[^{13}C] difference spectrum (see also Fig. 1A). Fig. 3 also shows the best fit of the measured ^{1}H-[^{13}C] NMR spectrum as well as the spectral contributions of glutamate, glutamine, GABA and lactate. Note that [2-^{13}C]-GABA appears as a clear upfield shoulder of the [4-^{13}C]-glutamate resonance. Repeating the spectral fit without the inclusion of [2-^{13}C]-GABA (data not shown) resulted in a significant residual, indicating that GABA is an essential part of the ^{1}H-[^{13}C] NMR spectrum.

Figure 4 shows typical turnover curves from a single animal for (A) [4-^{13}C] and [3-^{13}C]-glutamate, (B) [4-^{13}C] and [3-^{13}C]-glutamine and (C) [2-^{13}C] and [4-^{13}C]-GABA together with the best fit of the metabolic model described in the Methods section. Experimental data was averaged over 16 min in order to increase the SNR.

Figure 5 shows the endpoint ^{1}H-[^{13}C] spectrum acquired 120 min following the start of [2-^{13}C]-acetate infusion. Besides the large [2-^{13}C]-acetate resonance at 1.91 ppm, an increased [4-^{13}C]-glutamine resonance relative to the [4-^{13}C]-glutamate is characteristic, as has been shown previously by direct ^{13}C NMR detection (Bluml et al. 2002;Lebon et al. 2002). The [3-^{13}C]-GABA resonance was overwhelmed by the much larger [2-^{13}C]-acetate resonance and could not be quantified. The signal upfield from the [4-^{13}C]-Glu resonance can only be explained by the presence of [2-^{13}C]-GABA (dotted line). Omission of GABA leads to a strong degradation of the spectral fit.

From the steady-state [2-^{13}C]-acetate experiment, the ratio between V_{cycle} and V_{TCA} was determined for the glutamatergic ($V_{cycle,GluGln}/V_{TCA,Glu}$ = 0.58 ± 0.076) and GABAergic neurons ($V_{cycle,GABAGln}/V_{TCA,GABA}$ = 0.54 ± 0.063). The endpoint fractional enrichments for Glu-H4, Gln-H4 and GABA-H2 are 11.06 ± 1.50 %, 27.11 ± 3.68 % and 9.51 ± 1.49 %, respectively. These values were used to constrain the metabolic model during the fitting of the data obtained with [U-$^{13}C_6$]-glucose. The resulting TCA cycle rates were given by $V_{TCA,Glu}$ = 0.472 ± 0.040 μmol/min/g, $V_{TCA,GABA}$ = 0.062 ± 0.009 μmol/min/g and $V_{TCA,A}$ = 0.144 ± 0.025 μmol/min/g. Using the [2-^{13}C]-acetate data as constraint, the excitatory and inhibitory neurotransmitter cycle rates were given by $V_{cycle,GluGln}$ = 0.274 ± 0.023 μmol/min/g and $V_{cycle,GABAGln}$ = 0.033 ± 0.005 μmol/min/g, representing 89.2 % and 10.8 % of the total neurotransmitter cycling fluxes, respectively. The GABA shunt, V_{GABA}, was determined as 0.025 ± 0.006 μmol/min/g, whereas the exchange rate between α-KG and Glu, V_x, was 5.5 ± 2.4 μmol/min/g. The dilutional rates were all less than 0.065 μmol/min/g.

DISCUSSION

Here we have shown that the metabolic turnover of the excitatory and inhibitory neurotransmitters, glutamate and GABA, can be detected simultaneously by ^{1}H-[^{13}C]-NMR spectroscopy in rat brain *in vivo*. The infusion of [U-$^{13}C_6$]-glucose gives information about glutamatergic and GABAergic energy metabolism, as well as total neurotransmission. When

used in combination with steady-state fractional enrichments following a [2-^{13}C]-acetate infusion, the total neurotransmitter cycle rate can be separated into the glutamatergic and GABAergic contributions.

In the current study we were able to detect the fractional enrichment and concentration of cerebral glucose directly through a combination of selective heteronuclear editing and decoupling and very selective water suppression. The primary benefit of direct cerebral glucose detection is that no assumptions are necessary regarding blood-to-brain glucose transport kinetics. Furthermore, *in vivo* detection allows for a much higher temporal resolution than would be possible with arterial blood sampling.

While the results demonstrate the feasibility of detecting cerebral GABA turnover by ^{1}H-[^{13}C] NMR spectroscopy, the technique is demanding and optimal experimental conditions must be obtained for successful completion of the study. Foremost, the magnetic field homogeneity must be sufficient to allow the differentiation of glutamate-H4 and GABA-H2. At 9.4 T this condition required that the line width of water be no more than 16 Hz. Such a line width could only be achieved through the use of all first and second-order spherical harmonics shims in combination with stabile and optimal animal physiology. To account for temporal magnetic field drifts it was crucial to store each FID separately and perform a post-acquisition frequency correction prior to any further processing.

Besides optimal magnetic field homogeneity, the spectral SNR was also important for reliable GABA detection. Given a GABA concentration of 1.17 ± 0.31 mmol/L (Table 1) and an endpoint fractional enrichment of circa 35% during [U-$^{13}C_6$]-glucose infusion, the spectral sensitivity must be sufficient to detect 0.4 mM GABA in 16 min. The volume size of 180 μL at 9.4 T in the current study was sufficient to detect GABA turnover reliably. In future studies the volume size can potentially be decreased, especially when the magnetic field homogeneity over the smaller volume improves.

The spectral fitting algorithm yielded the total GABA concentration from the total, non-edited ^{1}H NMR spectrum, as was previously reported (Pfeuffer et al. 1999a). However, the non-edited GABA concentration (0.50 ± 0.07 mM) displayed a clear deviation from known GABA concentrations (0.83 – 2.30 mM, (Pfeuffer et al. 1999a)) in rat brain *in vivo*. The total GABA concentration (1.17 ± 0.31 mM) obtained by homonuclear spectral editing was in good agreement with literature values. The accuracy of the GABA concentration obtained by spectral editing was lower than that obtained by short TE NMR spectroscopy, likely due to a lower spectral SNR. However, the GABA extracted from short TE ^{1}H NMR spectra was biased towards a lower concentration. This can be attributed to significant spectral overlap of GABA at all spectral positions and a strong correlation between GABA and the macromolecular baseline (Ratiney et al. 2005). In contrast, the edited GABA ^{1}H NMR spectrum has no macromolecular baseline and minimal spectral overlap, such that the accuracy is directly related to the spectral SNR. Given the importance of the absolute GABA concentration, the reliability of homonuclear spectral editing was preferred over the precision of short TE MR spectra.

The value of $V_{cycle,GABAGln}$ = 0.033 ± 0.005 μmol/min/g is lower than a previous estimate by Patel et al. (Patel et al. 2005) of 0.135 ± 0.015 μmol/min/g measured for the rat cortex under similar physiological conditions (halothane anaesthesia). In contrast, Yang et al (Yang et al. 2007), using a selective inhibitor of GABA transaminase (gabaculine) to elevate the GABA pool and enhance ^{13}C label trapping from [1-^{13}C]-glucose, determined a value $V_{cycle,GABAGln}$ = 0.030 ± 0.007 μmol/min/g for the brain of α-chloralose anaesthetized rats. This value is consistent with previous estimates of GABA synthesis and $V_{cycle,GABAGln}$ after acute GABA-transaminase inhibition under similar physiological conditions (Mason et al.

2001), but is less than values determined in the absence of such inhibitors. The higher GABA turnover rate in our previous study (Patel et al. 2005) is likely to result from a higher fraction of pure cortical tissue, whereas the large 180 μL volume of the current study contains large amounts (> 60%) of white matter and subcortex, including corpus callosum, hippocampus and thalamus (Fig. 1B). The similarity in the present value of $V_{TCA,n}$ (= $V_{TCA,Glu}$ + $V_{TCA,GABA}$ = 0.53 μmol/g/min) to the subcortex (0.44 μmol/g/min), but not to the cortex (0.73 μmol/g/min) from a previous study (de Graaf et al. 2004) supports this contention.

Yang et al. (Yang et al. 2007) were not able to detect [2-^{13}C]-GABA labeling during [2-^{13}C]-acetate infusion under normal conditions (i.e. without vigabatrin). However, given the low GABA-H2 fractional enrichment and concentration and the 3.5 times smaller volume, the absence of [2-^{13}C]-GABA detection by Yang et al. (Yang et al. 2007) may simply be explained by an inadequate spectral SNR. Patel et al. (Patel et al. 2005) studied GABAergic neurotransmission in the rat cortex *ex vivo* and found significant GABA turnover from [2-^{13}C]-acetate ($V_{cycle,GABAGln}/V_{TCA,GABA}$ = 0.45), consistent with other studies reporting *ex vivo* measurements of GABA labeling from [1,2-$^{13}C_2$]-acetate in extracts of rat (Preece and Cerdan 1996) and mouse (Hassel et al. 1998) brain.

CONCLUSIONS

This work has shown that simultaneous detection of glutamatergic and GABAergic neurotransmission and the associated energy metabolism in rat brain *in vivo* is possible at 9.4 T under optimal experimental conditions. This capacity opens the possibility of studying excitatory and inhibitory neurotransmission during a wide range of conditions, including functional activation and neurological disorders, like epilepsy.

Acknowledgments

This research was supported by NIH grants R01 DK027121 (K. L. B.), K02 AA13420 (G. F. M.) and P30 NS052519 and a grant (NEF 04-15) from Hersenstichting Nederland (K. P. J. B.). The authors thank Bei Wang for expert animal preparation, Peter Brown for construction and maintenance of the ^{1}H-[^{13}C] RF coil and Terence Nixon and Scott McIntyre for system maintenance.

REFERENCES

Adriany G, Gruetter R. A half-volume coil for efficient proton decoupling in humans at 4 tesla. J Magn Reson 1997;125:178–184. [PubMed: 9245377]

Alcolea, A.; Carrera, J.; Medina, A. A hybrid Marquardt-simulated annealing method for solving the groundwater inverse problem; Proceedings of the ModelCARE 99 conference; IAHS publishing, Zurich, Switzerland. 1999; p. 157-163.

Beckmann N, Turkalj I, Seelig J, Keller U. ^{13}C NMR for the assessment of human brain glucose metabolism *in vivo*. Biochemistry 1991;30:6362–6366. [PubMed: 2054342]

Behar KL, Petroff OA, Prichard JW, Alger JR, Shulman RG. Detection of metabolites in rabbit brain by 13C NMR spectroscopy following administration of [1-13C]glucose. Magn Reson Med 1986;3:911–920. [PubMed: 2881185]

Bluml S, Moreno-Torres A, Shic F, Nguy CH, Ross BD. Tricarboxylic acid cycle of glia in the *in vivo* human brain. NMR Biomed 2002;15:1–5. [PubMed: 11840547]

Boumezbeur F, Besret L, Valette J, Gregoire MC, Delzescaux T, Maroy R, Vaufrey F, Gervais P, Hantraye P, Bloch G, Lebon V. Glycolysis versus TCA cycle in the primate brain as measured by combining ^{18}F-FDG PET and ^{13}C-NMR. J Cereb Blood Flow Metab 2005;25:1418–1423. [PubMed: 15917749]

Chaudhry FA, Lehre KP, van Lookeren Campagne M, Ottersen OP, Danbolt NC, Storm-Mathisen J. Glutamate transporters in glial plasma membranes: highly differentiated localizations revealed by quantitative ultrastructural immunocytochemistry. Neuron 1995;15:711–720. [PubMed: 7546749]

Chen W, Zhu XH, Gruetter R, Seaquist ER, Adriany G, Ugurbil K. Study of tricarboxylic acid cycle flux changes in human visual cortex during hemifield visual stimulation using ^{1}H-[^{13}C] MRS and fMRI. Magn Reson Med 2001;45:349–355. [PubMed: 11241689]

Chhina N, Kuestermann E, Halliday J, Simpson LJ, Macdonald IA, Bachelard HS, Morris PG. Measurement of human tricarboxylic acid cycle rates during visual activation by ^{13}C magnetic resonance spectroscopy. J Neurosci Res 2001;66:737–746. [PubMed: 11746397]

de Graaf RA. Theoretical and experimental evaluation of broadband decoupling techniques for in vivo NMR spectroscopy. Magn Reson Med 2005;53:1297–1306. [PubMed: 15906279]

de Graaf RA, Nicolay K. Adiabatic water suppression using frequency selective excitation. Magn Reson Med 1998;40:690–696. [PubMed: 9797151]

de Graaf RA, Patel AB, Rothman DL, Behar KL. Acute regulation of steady-state GABA levels following GABA-transaminase inhibition in rat cerebral cortex. Neurochem Int 2006a;48:508–514. [PubMed: 16517019]

de Graaf RA, Brown PB, Mason GF, Rothman DL, Behar KL. Detection of [1,6-$^{13}C_2$]-glucose metabolism in rat brain by *in vivo* ^{1}H-[^{13}C]-NMR spectroscopy. Magn Reson Med 2003;49:37–46. [PubMed: 12509818]

de Graaf RA, Mason GF, Patel AB, Rothman DL, Behar KL. Regional glucose metabolism and glutamatergic neurotransmission in rat brain in vivo. Proc Natl Acad Sci U S A 2004;101:12700–12705. [PubMed: 15310848]

de Graaf RA, Brown PB, McIntyre S, Nixon TW, Behar KL, Rothman DL. High magnetic field water and metabolite proton T_1 and T_2 relaxation in rat brain *in vivo*. Magn Reson Med 2006b;9

Deelchand DK, Shestov AA, Koski DM, Ugurbil K, Henry PG. Acetate transport and utilization in the rat brain. J Neurochem 2009a;109:46–54. [PubMed: 19393008]

Deelchand DK, Nelson C, Shestov AA, Ugurbil K, Henry PG. Simultaneous measurement of neuronal and glial metabolism in rat brain *in vivo* using co-infusion of [1,6-$^{13}C_2$]glucose and [1,2-$^{13}C_2$] acetate. J Magn Reson 2009b;196:157–163. [PubMed: 19027334]

Fitzpatrick SM, Hetherington HP, Behar KL, Shulman RG. The flux from glucose to glutamate in the rat brain *in vivo* as determined by ^{1}H-observed, ^{13}C-edited NMR spectroscopy. J Cereb Blood Flow Metab 1990;10:170–179. [PubMed: 1968068]

Fujiwara T, Nagayama K. Composite inversion pulses with frequency switching and their application to broadband decoupling. J Magn Reson 1988;77:53–63.

Gruetter R. Automatic, localized *in vivo* adjustment of all first- and second-order shim coils. Magn Reson Med 1993;29:804–811. [PubMed: 8350724]

Gruetter R, Seaquist ER, Ugurbil K. A mathematical model of compartmentalized neurotransmitter metabolism in the human brain. Am J Physiol Endocrinol Metab 2001;281:E100–112. [PubMed: 11404227]

Gruetter R, Novotny EJ, Boulware SD, Mason GF, Rothman DL, Shulman GI, Prichard JW, Shulman RG. Localized ^{13}C NMR spectroscopy in the human brain of amino acid labeling from D-[1-^{13}C] glucose. J Neurochem 1994;63:1377–1385. [PubMed: 7931289]

Haase A, Frahm J, Hanicke W, Matthaei D. 1H NMR chemical shift selective (CHESS) imaging. Phys Med Biol 1985;30:341–344. [PubMed: 4001160]

Hassel B, Johannessen CU, Sonnewald U, Fonnum F. Quantification of the GABA shunt and the importance of the GABA shunt versus the 2-oxoglutarate dehydrogenase pathway in GABAergic neurons. J Neurochem 1998;71:1511–1518. [PubMed: 9751184]

Henry PG, Russeth KP, Tkac I, Drewes LR, Andrews MT, Gruetter R. Brain energy metabolism and neurotransmission at near-freezing temperatures: *in vivo* ^{1}H MRS study of a hibernating mammal. J Neurochem 2007;101:1505–1515. [PubMed: 17437538]

Lebon V, Petersen KF, Cline GW, Shen J, Mason GF, Dufour S, Behar KL, Shulman GI, Rothman DL. Astroglial contribution to brain energy metabolism in humans revealed by ^{13}C nuclear magnetic resonance spectroscopy: elucidation of the dominant pathway for neurotransmitter glutamate repletion and measurement of astrocytic oxidative metabolism. J Neurosci 2002;22:1523–1531. [PubMed: 11880482]

Manor D, Rothman DL, Mason GF, Hyder F, Petroff OA, Behar KL. The rate of turnover of cortical GABA from [1-13C]glucose is reduced in rats treated with the GABA-transaminase inhibitor vigabatrin (gamma-vinyl GABA). Neurochem Res 1996;21:1031–1041. [PubMed: 8897466]

Mason GF, Behar KL, Rothman DL, Shulman RG. NMR determination of intracerebral glucose concentration and transport kinetics in rat brain. J Cereb Blood Flow Metab 1992;12:448–455. [PubMed: 1569138]

Mason GF, Petersen KF, de Graaf RA, Shulman GI, Rothman DL. Measurements of the anaplerotic rate in the human cerebral cortex using ^{13}C magnetic resonance spectroscopy and [1-^{13}C] and [2-^{13}C] glucose. J Neurochem 2007;100:73–86. [PubMed: 17076763]

Mason GF, Gruetter R, Rothman DL, Behar KL, Shulman RG, Novotny EJ. Simultaneous determination of the rates of the TCA cycle, glucose utilization, alpha-ketoglutarate/glutamate exchange, and glutamine synthesis in human brain by NMR. J Cereb Blood Flow Metab 1995;15:12–25. [PubMed: 7798329]

Mason GF, Falk Petersen K, de Graaf RA, Kanamatsu T, Otsuki T, Rothman DL. A comparison of ^{13}C NMR measurements of the rates of glutamine synthesis and the tricarboxylic acid cycle during oral and intravenous administration of [1-^{13}C]glucose. Brain Res Brain Res Protoc 2003;10:181–190. [PubMed: 12565689]

Mason GF, Martin DL, Martin SB, Manor D, Sibson NR, Patel A, Rothman DL, Behar KL. Decrease in GABA synthesis rate in rat cortex following GABA-transaminase inhibition correlates with the decrease in GAD(67) protein. Brain Res 2001;914:81–91. [PubMed: 11578600]

Mescher M, Merkle H, Kirsch J, Garwood M, Gruetter R. Simultaneous in vivo spectral editing and water suppression. NMR Biomed 1998;11:266–272. [PubMed: 9802468]

Patel AB, de Graaf RA, Mason GF, Rothman DL, Shulman RG, Behar KL. The contribution of GABA to glutamate/glutamine cycling and energy metabolism in the rat cortex in vivo. Proc Natl Acad Sci U S A 2005;102:5588–5593. [PubMed: 15809416]

Patel AB, de Graaf RA, Mason GF, Kanamatsu T, Rothman DL, Shulman RG, Behar KL. Glutamatergic neurotransmission and neuronal glucose oxidation are coupled during intense neuronal activation. J Cereb Blood Flow Metab 2004;24:972–985. [PubMed: 15356418]

Pfeuffer J, Tkac I, Provencher SW, Gruetter R. Toward an *in vivo* neurochemical profile: quantification of 18 metabolites in short-echo-time ^{1}H NMR spectra of the rat brain. J Magn Reson 1999a;141:104–120. [PubMed: 10527748]

Pfeuffer J, Tkac I, Choi IY, Merkle H, Ugurbil K, Garwood M, Gruetter R. Localized *in vivo* ^{1}H NMR detection of neurotransmitter labeling in rat brain during infusion of [1-^{13}C] D-glucose. Magn Reson Med 1999b;41:1077–1083. [PubMed: 10371437]

Preece NE, Cerdan S. Metabolic precursors and compartmentation of cerebral GABA in vigabatrin-treated rats. J Neurochem 1996;67:1718–1725. [PubMed: 8858958]

Provencher SW. Estimation of metabolite concentrations from localized *in vivo* proton NMR spectra. Magn Reson Med 1993;30:672–679. [PubMed: 8139448]

Ratiney H, Sdika M, Coenradie Y, Cavassila S, van Ormondt D, Graveron-Demilly D. Time-domain semi-parametric estimation based on a metabolite basis set. NMR Biomed 2005;18:1–13. [PubMed: 15660450]

Rothman DL, Behar KL, Hetherington HP, den Hollander JA, Bendall MR, Petroff OA, Shulman RG. ^{1}H-Observe/^{13}C-decouple spectroscopic measurements of lactate and glutamate in the rat brain *in vivo*. Proc Natl Acad Sci U S A 1985;82:1633–1637. [PubMed: 2858850]

Rothman DL, Novotny EJ, Shulman GI, Howseman AM, Petroff OA, Mason G, Nixon T, Hanstock CC, Prichard JW, Shulman RG. ^{1}H-[^{13}C] NMR measurements of [4-^{13}C]glutamate turnover in human brain. Proc Natl Acad Sci U S A 1992;89:9603–9606. [PubMed: 1409672]

Shen J, Petersen KF, Behar KL, Brown P, Nixon TW, Mason GF, Petroff OA, Shulman GI, Shulman RG, Rothman DL. Determination of the rate of the glutamate/glutamine cycle in the human brain by *in vivo* ^{13}C NMR. Proc Natl Acad Sci U S A 1999;96:8235–8240. [PubMed: 10393978]

Sibson NR, Dhankhar A, Mason GF, Behar KL, Rothman DL, Shulman RG. *In vivo* ^{13}C NMR measurements of cerebral glutamine synthesis as evidence for glutamate-glutamine cycling. Proc Natl Acad Sci U S A 1997;94:2699–2704. [PubMed: 9122259]

Sibson NR, Dhankhar A, Mason GF, Rothman DL, Behar KL, Shulman RG. Stoichiometric coupling of brain glucose metabolism and glutamatergic neuronal activity. Proc Natl Acad Sci U S A 1998;95:316–321. [PubMed: 9419373]

Sibson NR, Mason GF, Shen J, Cline GW, Herskovits AZ, Wall JE, Behar KL, Rothman DL, Shulman RG. *In vivo* ^{13}C NMR measurement of neurotransmitter glutamate cycling, anaplerosis and TCA cycle flux in rat brain during [2-^{13}C]-glucose infusion. J Neurochem 2001;76:975–989. [PubMed: 11181817]

Storm-Mathisen J, Leknes AK, Bore AT, Vaaland JL, Edminson P, Haug FM, Ottersen OP. First visualization of glutamate and GABA in neurones by immunocytochemistry. Nature 1983;301:517–520. [PubMed: 6130475]

Tannus A, Garwood M. Improved performance of frequency-swept pulses using offset-independent adiabaticity. J Magn Reson A 1996;120:133–137.

Yang J, Li SS, Bacher J, Shen J. Quantification of cortical GABA-glutamine cycling rate using *in vivo* magnetic resonance signal of [2-^{13}C]GABA derived from glia-specific substrate [2-^{13}C]acetate. Neurochem Int 2007;50:371–378. [PubMed: 17056156]

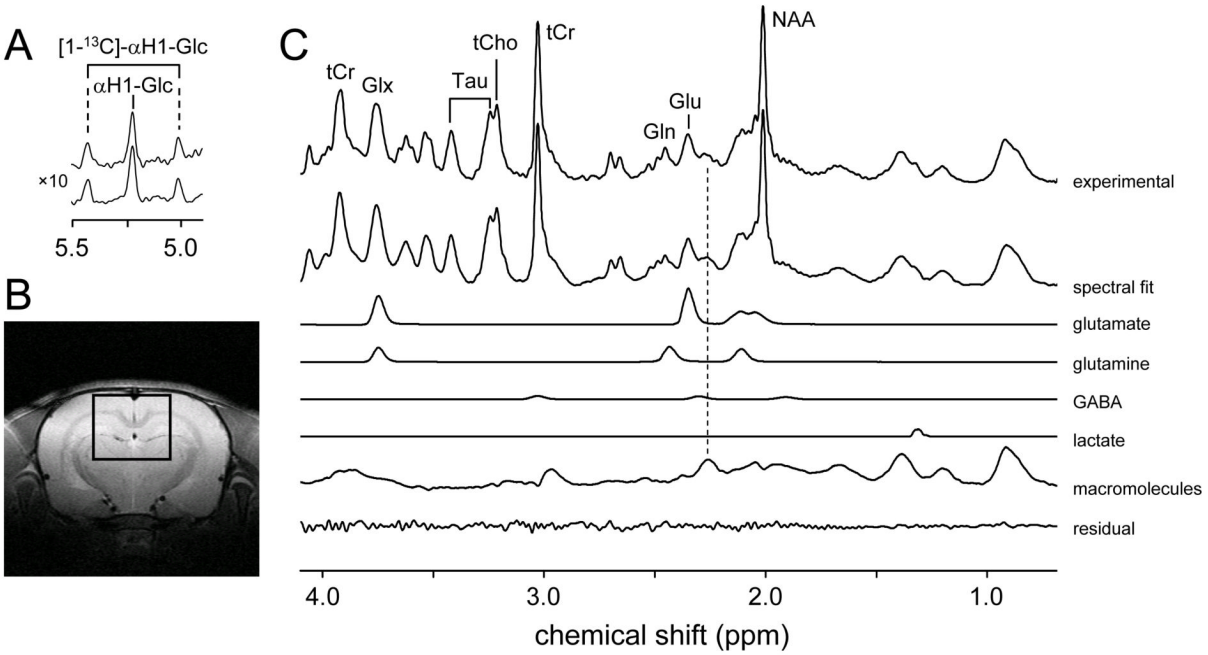

Figure 1.

Localized ^{1}H-[^{13}C] NMR spectroscopy of rat brain *in vivo* at 9.4 T acquired between 120 and 150 min following the start of intravenous [U-$^{13}C_6$]-glucose infusion. (A) The [1-^{12}C]-αH1-glucose signal appears at 5.22 ppm, whereas the [1-^{13}C]-αH1-glucose signal appears, due to selective decoupling, as a doublet signal with a one-bound ^{1}H-^{13}C scalar coupling of 169 Hz. Due to selective spectral editing, the proton glucose resonances are identical in the absence (upper trace) and presence (lower trace) of the ^{13}C inversion pulse. (B) Location of the 180 μL (= 6 × 5 × 6 mm) voxel. (C) Experimental ^{1}H NMR spectrum averaged over 32 min in the absence of a ^{13}C inversion pulse (top trace), together with the total spectral fit, the spectral contributions of glutamate, glutamine, GABA, lactate and macromolecules to the total spectral fit and the difference between the experimental and fitted ^{1}H NMR spectra (lower trace). Abbreviations: Glx, sum of Gln and Glu; tCho, total choline representing the sum of GPC and PC; tCr, total creatine respresenting the sum of Cr and PCr.

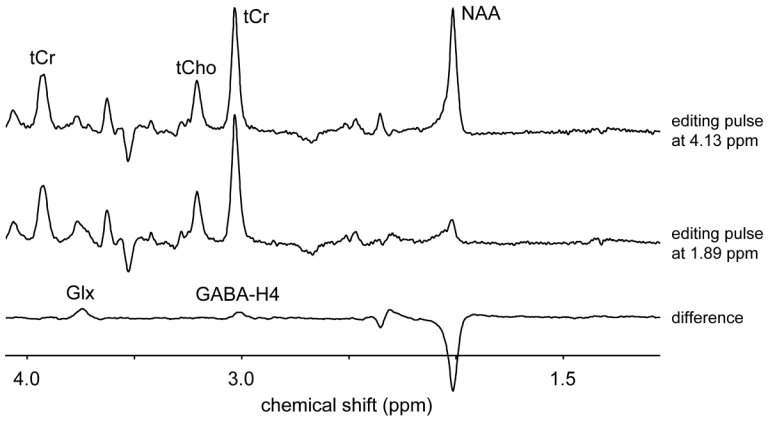

Figure 2.

Spectral editing of GABA in rat brain *in vivo* at 9.4 T. ^{1}H NMR spectra are acquired in which the 20 ms Gaussian editing pulses selectively refocus the GABA-H3 resonance at 1.89 ppm (middle trace) or at a control position (4.13 ppm, upper trace) mirrored relative to the total creatine resonance at 3.01 ppm. The difference spectrum displays the edited GABA-H4 resonance at 3.01 ppm together with co-edited signals from glutamate/glutamine-H2, GABA-H2 and *N*-acetyl aspartate.

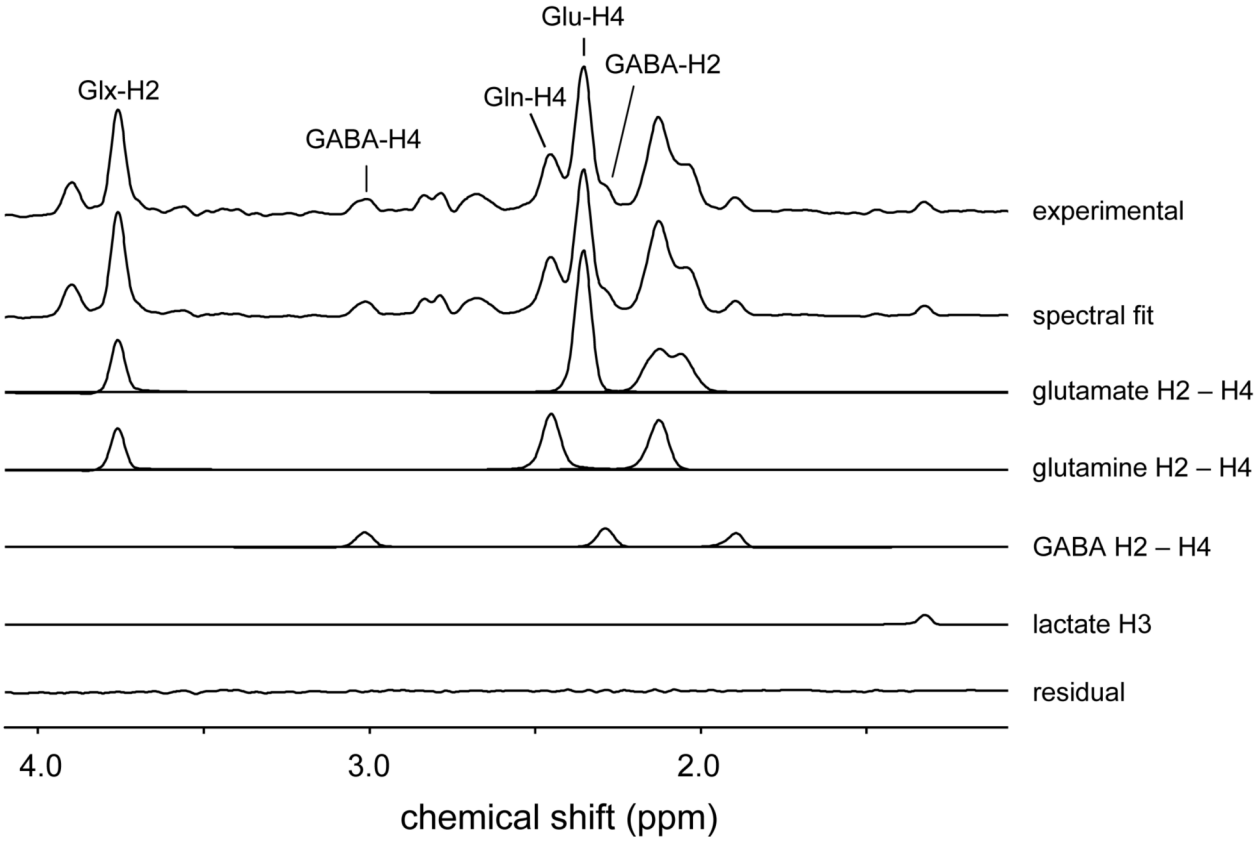

Figure 3.

Localized ^{1}H-[^{13}C] NMR spectroscopy of rat brain *in vivo* at 9.4 T acquired between 120 and 150 min following the start of intravenous [U-$^{13}C_6$]-glucose infusion. The ^{13}C-edited ^{1}H NMR spectrum is shown (top trace), together with the total spectral fit, as well as the spectral contribution of the glutamate, glutamine, GABA and lactate resonances to the total fit. The lower trace shows the difference between the experimental and fitted ^{13}C-edited ^{1}H NMR spectra.

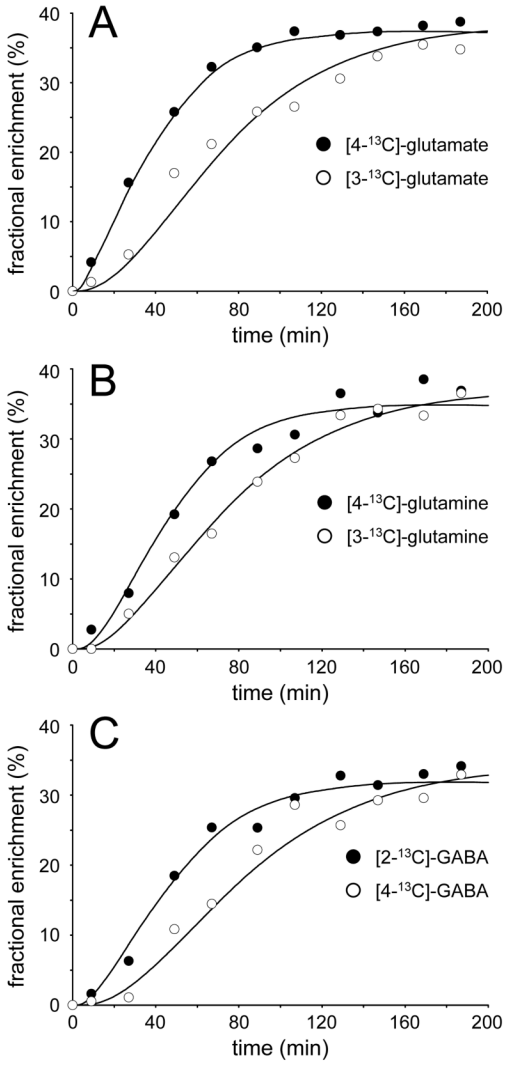

Figure 4.

Metabolic turnover curves for (A) [3-^{13}C] and [4-^{13}C]-glutamate, (B) [3-^{13}C] and [4-^{13}C]-glutamine and (C) [2-^{13}C] and [4-^{13}C]-GABA during the infusion of [U-$^{13}C_6$]-glucose. The dots represent the experimentally measured fractional enrichment, whereas the solid curves represent the best fit to the metabolic model.

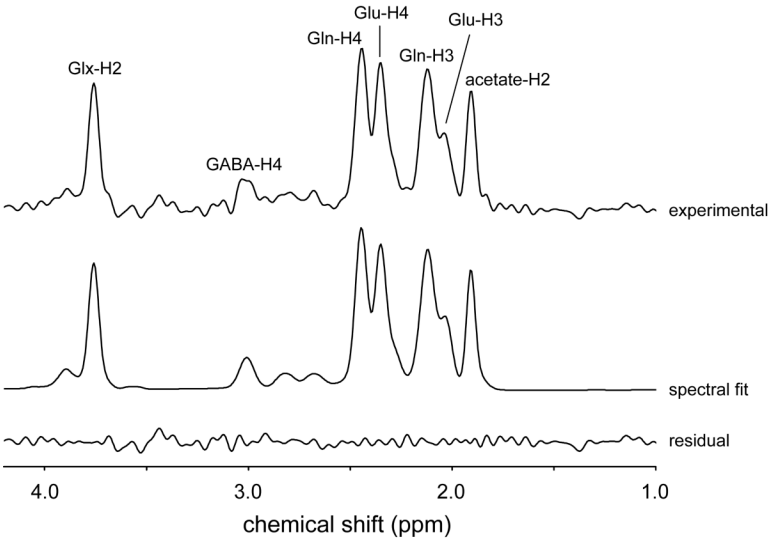

Figure 5.

Localized ^{1}H-[^{13}C] NMR spectroscopy of rat brain *in vivo* at 9.4 T following intravenous [2-^{13}C]-acetate infusion. The ^{13}C-edited ^{1}H NMR spectrum is shown (top trace), together with the total spectral fit, the spectral contributions of the H2, H3 and H4 label positions of glutamate, glutamine and GABA, the spectral contribution of acetate and the difference between the experimental and fitted ^{13}C-edited ^{1}H NMR spectra (lower trace). The experimental data (top trace) is averaged between 120 and 150 min following the onset of [2-^{13}C]-acetate infusion.

Table 1

Metabolite concentrations in rat brain obtained prior to intravenous substrate infusion[1]

		mean (mM)	SD (mM)	MCS (%)
alanine		0.27	0.09	58.30
aspartate		2.48	1.00	11.89
choline (total)		1.71	0.09	9.90
	GPC	0.99	0.08	11.59
	PC	0.72	0.06	24.88
GABA [2]		1.17	0.31	16.68
glutamate		10.11	0.93	4.67
glutamine		4.56	0.53	7.30
glutathione		1.98	1.28	9.77
myo-inositol		3.84	0.48	3.15
NAA		8.95	0.44	1.26
NAAG		2.90	0.69	13.58
lactate		0.82	0.15	30.08
PE		1.58	0.11	10.48
taurine		3.54	0.11	4.06
valine		0.39	0.07	20.81

[1] All concentrations are referenced to 10 mM total creatine (n = 10).

[2] Obtained from J-difference edited ^{1}H NMR spectra.